Naunyn-Schmiedeberg's Archives of Pharmacology (2024) 397:1727–1736
https://doi.org/10.1007/s00210-023-02708-x

RESEARCH

Proprotein convertase subtilisin/kexin 9 inhibitor downregulates microRNA-130a-3p expression in hepatocytes to alleviates atherosclerosis progression

Jinghan Xu[1,2,3,4] · Junrong Zuo[5] · Chuyi Han[1,2,3,4] · Tingting Li[1,2,3,4] · Dongxia Jin[1,2,3,4] · Fumei Zhao[1,2,3,4] · Hongliang Cong[1,2,3,4]

Received: 16 June 2023 / Accepted: 3 September 2023 / Published online: 15 September 2023

Abstract

Proprotein convertase subtilisin/kexin 9 (PCSK9) inhibitors have been shown to regulate lipid metabolism and reduce the risk of cardiovascular events. This study explores the effect and potential mechanism of PCSK9 inhibitors on lipid metabolism and coronary atherosclerosis. HepG2 cells were incubated with PCSK9 inhibitor. ApoE-/- mice were fed with a high fat to construct an atherosclerosis model, and then treated with PCSK9 inhibitor (8 mg/kg for 8 w). PCSK9 inhibitor down-regulated microRNA (miRNA)-130a-3p expression in a dose-dependent manner. And, miR-130a-3p could bind directly to the 3' untranslated region (3'-UTR) region of LDLR to down-regulate LDLR expression in HepG2 cells, as confirmed by the luciferase reporter gene assay. In addition, miR-130a-3p overexpression significantly attenuated the promoting effect of PCSK9 inhibitor on LDLR and DiI-LDL uptake in HepG2 cells. More importantly, in vivo experiments confirmed that PCSK9 inhibitor could significantly inhibit miR-130a-3p levels and promote LDLR expression in liver tissues, thus regulating serum lipid profile and alleviating the progression of coronary atherosclerosis. PCSK9 inhibitor could moderately improve coronary atherosclerosis by regulating miR-130a-3p/LDLR axis, providing an exploitable strategy for the treatment of coronary atherosclerosis.

Keywords PCSK9 inhibitor · Atherosclerosis · miRNA-130a-3p · LDLR

Background

Atherosclerosis and its associated atherosclerotic cardiovascular disease (ASCVD) are the leading cause of death worldwide (Förstermann et al. 2017). Dyslipidemia, characterized by increased level of total cholesterol and low-density lipoprotein cholesterol (LDL-C) and reduced level of high-density lipoprotein cholesterol (HDL-C), has been identified as a pathogenic risk factor of ASCVD, which is closely related to the risk and severity of ASCVD (Hilvo and Dhar 2022). Lipid-lowering therapy can effectively prevent or reduce cardiovascular and peripheral adverse events and improve cardiovascular outcomes in patients with ASCVD (Sánchez-Bacaicoa et al. 2022). PCSK9 inhibitors are an effective and most used drugs in clinical lipid-lowering therapy (Aguilar-Salinas and Gómez-Díaz 2021; Oleaga et al. 2021). Some studies have found that one of the mechanism of PCSK9 inhibitors is to inhibit the binding of PCSK9 with LDL-receptors and prevent the degradation of LDL-receptors. However, many of the potential mechanisms of action by which PCSK9 inhibitors lower lipid remain to be further explored.

MiRNAs are small non-coding RNAs involved in the regulation of post-transcriptional gene expression (Suvorov et al. 2020). They promote degradation or inhibit translation of target genes by fully or incompletely pairing with the 3'UTR region of target genes,

✉ Hongliang Cong
doctor0618@163.com

1 The Department of Cardiology, Tianjin Chest Hospital, No. 261, Taierzhuang South Road, Jinnan District, Tianjin 300222, China

2 The Department of Cardiology, Chest Hospital, Tianjin University, Tianjin, China

3 Tianjin Key Laboratory of Cardiovascular Emergency and Critical Care, Tianjin Municipal Science and Technology Bureau, Tianjin, China

4 TianJin Institute of Cardiovascular Diseases, Tianjin, China

5 Internal Medicine, Tianjin Jinnan Hospital, Tianjin, China

and are involved in the regulation of ontogeny, apoptosis, proliferation and differentiation. A growing body of miRNAs have been confirmed to participate in the regulation of hepatic lipid homeostasis (Agbu and Carthew 2021). Moreover, miRNAs mediate pleiotropic effects of lipid-lowering drugs and are implicated in the variations in the lipid-lowering response (Leal et al. 2021; Saavedra et al. 2022). For example, miR-33b may affect the response to atorvastatin treatment (Ubilla et al. 2021). MiR-130a-3p plays a crucial role in the regulation of glucose and lipid metabolism. Wu J et al. (Wu et al. 2020) found that miR-130a-3p derived from liver exosomes alleviates glucose intolerance by downregulating PHLPP2 in adipocytes. Xiao et al. (Xiao et al. 2014) provided evidence showing a crucial role of miR-130a-3p in regulating insulin sensitivity and hepatic steatosis. In addition, miR-130a-3p is also an important regulatory molecule in liver fibrosis and steatohepatitis. Liu L et al. (Liu et al. 2021) reported that overexpression of miR-130a-3p could inhibit liver fibrosis. Wang Y et al. (Wang et al. 2017) demonstrated that miR-130a-3p promoted apoptosis of hepatic stellate cells in nonalcoholic fibrosis steatohepatitis. However, the effect of PCSK9 inhibitors on miRNA-dependent modulators in the regulation of lipid metabolism is largely undefined.

In this study, we hypothesized that PCSK9 inhibitor regulates lipid metabolism by modulating miR-130a-3p. To verify this hypothesis, we investigated the effect of PCSK9 inhibitor on miR-130a-3p expression and the relationship between miR-130a-3p and LDLR. Besides, rescue experiments investigated the role of miR-130a-3p in PCSK9 inhibitor-mediated LDLR expression and DiI-LDL uptake in HepG2 cells, and LDLR expression in liver tissues, serum lipid profile, and arterial atherosclerosis in vivo.

Methods and materials

Cells and cell culture

HepG2 cells were obtained from the Cell Bank of Shanghai Institute of Cell Biology, Chinese Academy of Sciences. Cells were cultured in Dulbecco's Modified Eagle Medium (DMEM) containing 10% fetal bovine serum (Gibico) at 37 °C with 5% CO_2.

PCSK9 inhibitor SBC-115076 (Catalog number: S7976) was obtained from Selleck Chemicals (Houston, TX, USA). HepG2 cells were incubated with different concentrations of SBC-115076 for 24 h.

QRT-PCR

Total RNA (RNAiso Plus, TaKaRa) was isolated from tissues or cells. The purity of RNA was determined using a NanoDrop spectrophotometer and the OD_{260}/OD_{280} ratio was 1.7 ~ 2.0. PrimeScript™ RT Reagent Kit (TaKaRa) was used for the synthesis of cDNA from total RNA samples. The purity of cDNA was assessed using gel electrophoresis and PCR of the housekeeping gene GAPDH. SYBR Premix Ex Taq ™ (TaKaRa, Dalian, China) was used for PCR reaction, and the PCR reaction mix including SYBR Premix Ex Taq II (2×) 10 uL, Forward Primer (10 uM) 0.8 uL, Reverse Primer (10 uM) 0.8 uL, cDNA 2 uL, ROX Reference Dye or Dye II (50×) 0.4 uL and Rnase-free water 6 uL. PCR reaction conditions were set as follows: 95℃ 30 s, followed by 40 cycles of 95℃ 5 s and 60℃ 30 s, then 95℃ 15 s, 60℃ 30 s, 95℃ 15 s.

The relative expression levels of PCSK9, LDLR, and miRNAs were analyzed by the $2^{-\Delta\Delta Ct}$ method. The primers were provided by Sangon Biotech (Shanghai), and their sequences were listed in Table 1.

Table 1 The sequences of primers used for qRT-PCR in this study

Gene name	Primer forward sequence (5′-3′)	Primer reverse sequence (5′-3′)
hsa-miR-19a-3p	TGCGGTGTGCAAATCTATGCAAA	CCAGTGCAGGGTCCGAGGT
hsa-miR-301a-3p	TGCGGCAGTGCAATAGTATTGTC	CCAGTGCAGGGTCCGAGGT
hsa-miR-152-3p	TGCGGTCAGTGCATGACAGAACT	CCAGTGCAGGGTCCGAGGT
hsa-miR-454-3p	TGCGGTAGTGCAATATTGCTTAT	CCAGTGCAGGGTCCGAGGT
hsa-miR-130a-3p	TGCGGCAGTGCAATGTTAAAAGG	CCAGTGCAGGGTCCGAGGT
mmu-miR-130a-3p	TGCGGCAGTGCAATGTTAAAAGG	CCAGTGCAGGGTCCGAGGT
U6	GCTCGCTTCGGCAGCACA	AACGCTTCACGAATTTGCGTG
PCSK9	GGAACCTGGAGCGGATTACC	CCCGGTGGTCACTCTGTATG
LDLR	CGTGAACCTGGAGGGTGGCT	GTGAAGAAGAGGTAGGCGATGGAG
GAPDH	ATGACATCAAGAAGGTGGTGAAGCAGG	GCGTCAAAGGTGGAGGAGTGGGT

Western blot

Proteins were isolated from cell lysates or liver tissues (30 µg) and transferred to the PVDF membrane. The membrane was incubated with specific antibodies of LDLR, PCSK9, and GAPDH at 4 °C overnight, respectively. Then, the membrane was incubated with a secondary antibody. The strips were visualized using an enhanced ECL system (Thermo Fisher, USA). Anti-PCSK9 antibody (ab185194) and anti-LDLR antibody were obtained from Abcam, and GAPDH from Immunoway (Suzhou, China).

Cell transfection

miR-130a-3p mimic and inhibitor, and their negative control (NC), were provided by GenePharma (Shanghai, China). The sequences were shown in Table 1. These plasmids are transfected in HepG2 cells using Lipofectamine 3000 Reagent (Invitrogen, USA).

Uptake of DiI-LDL assay

Uptake of DiI-LDL assay was performed according to the previous description (Xu et al. 2021). HepG2 cells were cultured in DMEM containing 2% LPDS and 20 µg/mL DiI-LDL at 37 °C for 4 h under dark conditions. The cells were then washed with PBS containing 0.4% albumin two times and PBS three times. Under a fluorescence microscope, the cells were fixed with 4% formalin and the nuclei were subsequently stained with DAPI. For fluorescence quantification, cells were incubated with isopropyl alcohol at room temperature for 20 min by shaking. 200 µL isopropyl samples were then used for analysis using a microplate reader. The remaining cells were lysed with NaOH (0.5 mol/L) for 30 min and 10 µL equal samples were taken to determine the protein (Bio-RAD, USA).

Luciferase reporter assay

Luciferase reporter assay was used to verify the targeting effect of miR-130a-3p and LDLR in HepG2 cells, according to a previous study (Zhou and Yang 2022).

Modeling and grouping

ApoE-knockout C57BL/6 mice were fed with a high fat to construct an atherosclerosis model. Twenty-four apoE-/- mice were divided into 4 groups with 6 mice in each group by random number table method. ApoE -/- mice were classified as follows: apoE-/- mice (model group), model group + PCSK9 inhibitor, model group + PCSK9 inhibitor + AAV-control, model group + PCSK9 inhibitor + AAV-miR-130a-3p. ApoE-/- mice of the same age were fed with a normal diet as the control group (control group, $n = 6$). Adenovirus AAV-control and AAV-miR-130a-3p were injected twice through the tail vein at 2×10^{12} µg/ body weight (g). From the 8th week, the mice that showed abnormal lipid levels were subcutaneously injected with PCSK9 inhibitor (8 mg/kg) twice a week and were sacrificed after 16 weeks of a high-fat diet.

The liver and descending aorta were removed and fixed. The liver was used for immunofluorescence and immunohistochemistry studies. The whole descending aorta was stained with oil red O, and the aortic root was stained with HE and oil red O.

Enzyme-linked immunosorbent assay

Mice were anesthetized with 2% pentobarbital sodium. After the eyeball was removed and euthanized, blood was collected from the posterior orbital sinus. The blood was placed for 2 h and centrifuged. The supernatant was collected and used for ELISA. The serum TC, TG, HDL-C, and ox-LDL levels were measured using corresponding assay kits as described previously (Jiang et al. 2022). The OD value of each sample at 450 nm was measured. Then, the linear standard curve was drawn according to the concentration of the standard substance and the corresponding OD value. The concentration of each sample was calculated according to the curve equation. TC, TG, and HDL-C assay kits were obtained from Jiancheng Biotechnology (Nanjing, China) and mouse ox-LDL Assay Kit was obtained from Kenuodi (Quanzhou, China).

Assess atherosclerotic lesions throughout the aorta

Facial lesions with oil red O staining of the entire aorta were quantified to determine the extent of atherosclerosis as described previously (Liu et al. 2022). In short, fat and connective tissue attached to the outer membrane were quickly removed under a stereoscopic microscope. The entire aorta from the arch to the iliac bifurcation was carefully removed, lengthways opened, stapled flat, and fixed overnight in 4% paraformaldehyde solution. The aorta was then rinsed with distilled water 3 times and stained with 0.5% ORO solution at room temperature for 2 h. The aorta was then discolored in 70% ethanol and rinsed with distilled water. Taken with a digital camera, the atherosclerotic plaque is stained red. The extent of AS was assessed using the percentage of the ORO-positive staining red area relative to the total aortic lumen surface area and quantified using Image-Pro plus6.0 software (Media Cybernetics, USA).

Morphological and histological analysis

The liver and aorta tissues of mice were dissected and placed in 4% paraformaldehyde overnight. The tissue was then embedded in a compound at the optimum cutting temperature and frozen at -80 °C for the next step. To measure lipid deposition in the sinus of the aorta, 8 μm thick sections were frozen with a cryothermostat and the cross-sections were stained with ORO.

Paraffin sections of the sinus of the aorta were made following previous protocols. In summary, the liver and aorta of mice were dissected and placed in 4% paraformaldehyde overnight. The tissue is then embedded in the compound at the optimum cutting temperature and frozen at −80 °C for further use. The sections with a thickness of 8 μm were frozen with a cryostat to measure lipid deposition in the sinus of the aorta and ORO staining was performed.

Statistical analysis

Data were analyzed by SPSS22.0 software. The numerical data were expressed as mean ± standard deviation ($\bar{x}\pm s$). Kolmogorov-Smirnov D was used to test the normal distribution of continuous variables. Analysis of variance was used for classification data of repeated measurements. Multiple random sets were compared using one-way ANOVA, and then any two groups of student-Newman-Keuls (SNK) were compared. A *P*-value of 0.05 was considered a statistically significant difference. Data were plotted using GraphPad Prism 8 Project software.

Results

PCSK9 inhibitor promotes LDLR and reduces miR-130a-3p expression in HepG2 cells

As expected, PCSK9 inhibitor reduced PCSK9 protein expression and promoted LDLR protein expression in a dose-dependent manner (Fig. 1A). Interestingly, PCSK9 inhibitor also significantly promoted LDLR expression at the transcriptional level (Fig. 1B). Further, we detected the abundance of several miRNAs that potentially modulate LDLR in HepG2 cells exposed to PCSK9 inhibitor. RT-PCR analysis showed that PCSK9 inhibitor reduced miR-130a-3p levels in a dose-dependent manner (Fig. 1C).

LDLR is a direct target of miR-130a-3p

To determine the regulatory between miR-130a-3p and LDLR, the wild-type 3'-UTR sequence of LDLR mRNA (LDLR 3'-UTR-wt) or mutated sequence (LDLR 3'-UTR-mut) were inserted into the Luciferase reporter vector and then transfected with miR-130a-3p mimics into HepG2 cells (Fig. 2A). As displayed in Fig. 2B, miR-130a-3p mimics transfection significantly suppressed the luciferase activity of LDLR 3'-UTR-wt plasmids, but had no influence on the luciferase activity of LDLR 3'-UTR-mut plasmids. In addition, HepG2 cells were transfected with miR-130a-3p mimics or inhibitors. It was found that miR-130a-3p mimics increased the endogenous miR-130a-3p expression

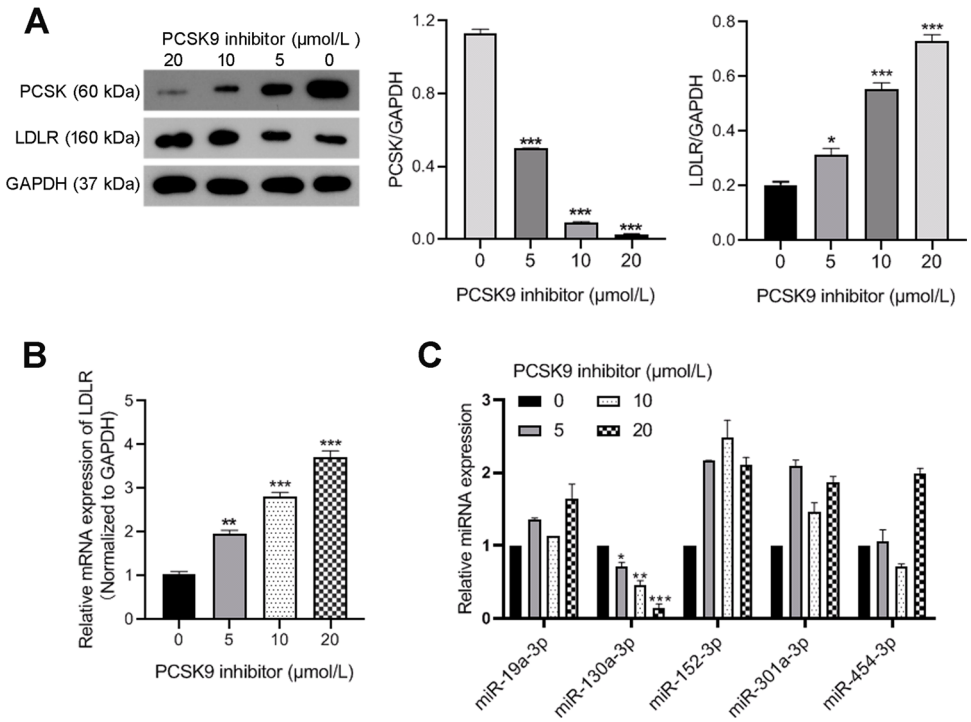

Fig. 1 Expression of PCSK9, LDLR, and miRNAs in HepG2 cells treated with PCSK9 inhibitor. HepG2 cells were treated with 0, 5, 10, and 20 μmol/L PCSK9 inhibitor, then total RNAs and protein were collected for experiments. **A** Expression of PCSK9 and LDLR proteins was detected via western blot. **B** The expression of LDLR mRNA was assessed by qRT-PCR. **C** The expression of miRNAs was assessed by qRT-PCR. Data present mean ± SEM from three independent experiments at least. **P* < 0.05; ***P* < 0.01; ****P* < 0.001, compared with the 0 groups

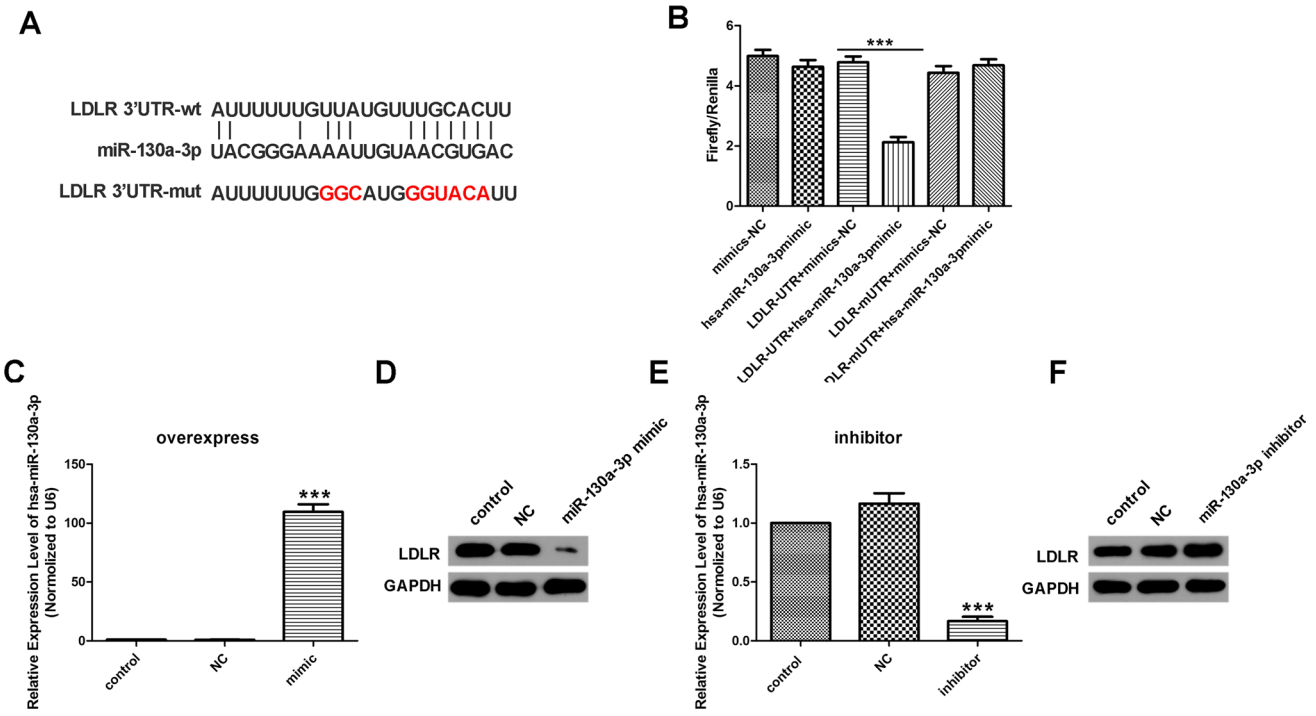

Fig. 2 LDLR is a direct target of miR-130a-3p. **A** The conserved binding sites of miR-130a-3p on LDLR mRNA 3'-UTR were predicted by StarBase. **B** Luciferase activity of WT-LDLR, but not the MUT-LDLR was evaluated in HepG2 cells co-transfected with miR-130a-3p mimics. **C** Expression of miR-130a-3p in HepG2 cells transfected with miR-130a-3p mimics. **D** Expression of LDLR in HepG2 cells transfected with miR-130a-3p mimics. **E** Expression of miR-130a-3p in HepG2 cells transfected with miR-130a-3p inhibitors. **F** Expression of LDLR in HepG2 cells transfected with miR-130a-3p inhibitors. Data present mean ± SEM from three independent experiments at least. ***$P < 0.001$, compared with the control groups

(Fig. 2C) and reduced LDLR levels (Fig. 2D). Meanwhile, miR-130a-3p or inhibitors decreased the endogenous miR-130a-3p expression (Fig. 2E) and promoted LDLR expression (Fig. 2F). These observations indicate that miR-130a-3p directly targets LDLR to inhibit its expression.

PCSK9 inhibitor downregulates miR-130a-3p to promote LDLR expression

To examine the role of miR-130a-3p in PCSK9-mediated effects, HepG2 cells were simultaneously treated with miR-130a-3p mimics and PCSK9 inhibitor. As displayed in Fig. 3A, PCSK9 inhibitor reduced miR-130a-3p expression, while transfection with miR-130a-3p mimic caused a significant increase of miR-130a-3p compared with the PCSK9 inhibitor alone. Meanwhile, PCSK9 inhibitor promoted LDLR mRNA and protein, which was partially eliminated by miR-130a-3p mimics (Fig. 3B and C). In atherosclerosis model mice, it was found that the expression of miR-130a-3p was increased in the liver tissue of atherosclerosis model mice. PCSK9 inhibitor reduced the expression of miR-130a-3p, while AAV-miR-130a-3p co-treatment re-increased miR-130a-3p compared with the PCSK9 inhibitor group ($P = 0.003$, Fig. 3D). LDLR expression was downregulated in liver tissues of atherosclerosis model mice, and PCSK9 inhibitor promoted LDLR expression, which was reversed by AAV-miR-130a-3p treatment (Fig. 3E). Furthermore, immunofluorescence staining also showed similar change of miR-130a-3p and LDLR expression (Fig. 3F). These data indicate that PCSK9 inhibitor promotes LDLR expression via downregulation of miR-130a-3p.

PCSK9 inhibitor promotes DiI-LDL uptake in HepG2 cells via regulation of miR-130a-3p

As shown in Fig. 4, PCSK9 inhibitor increased DiI-LDL uptake, while miR-130a-3p overexpression attenuated upregulated DiI-LDL uptake induced by PCSK9 inhibitor. These observations indicated that miR-130a-3p partially mediated LDLR expression and DiI-LDL uptake in HepG2 cells exposed to PCSK9 inhibitor.

PCSK9 inhibitor regulates serum lipid profile in mice via regulation of miR-130a-3p

Serum lipid profiles, including TG, TC, LDL-C, and HDL-C in each group were detected by ELISA. The levels of serum TG, TC, and LDL-C were increased and HDL-C

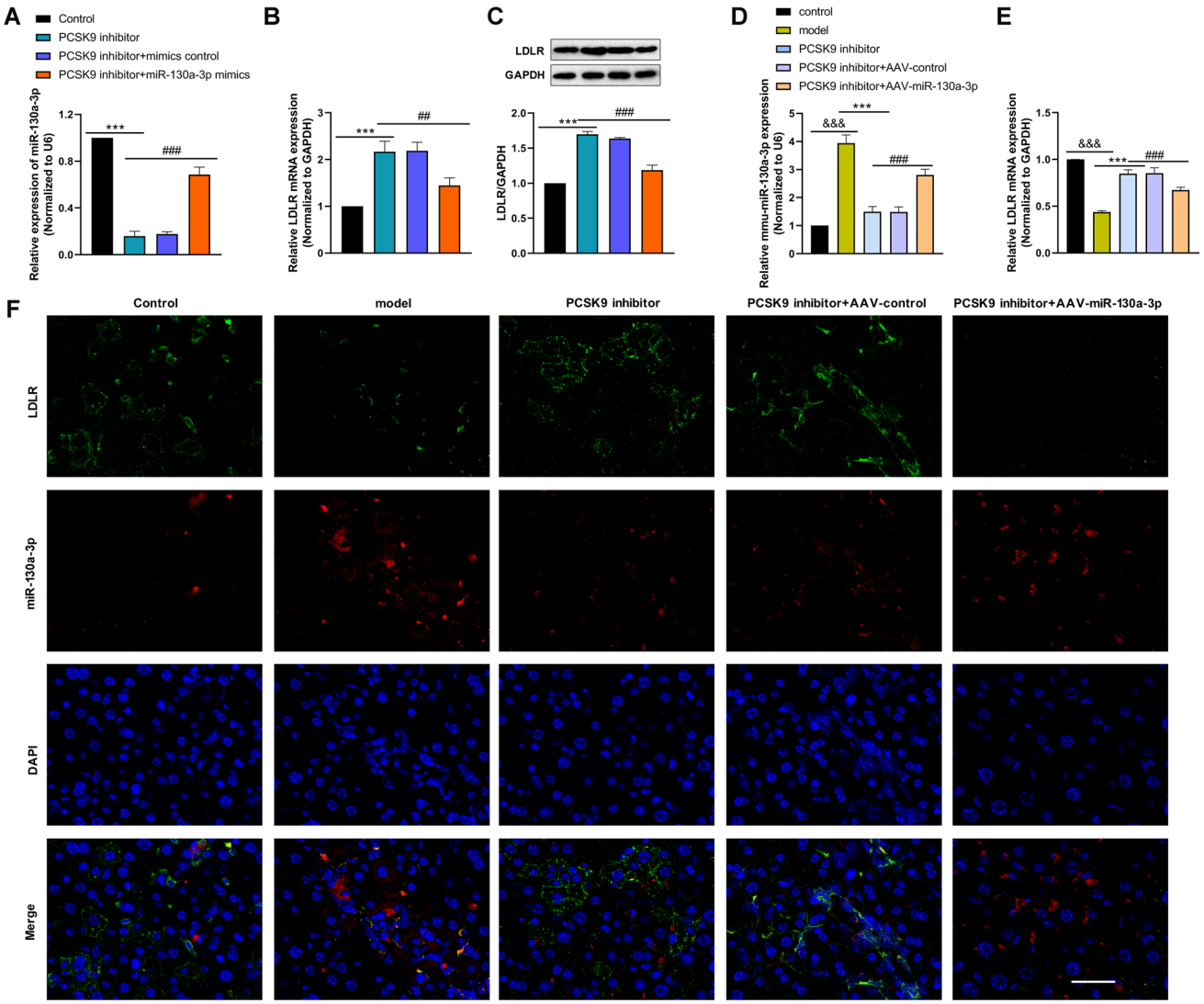

Fig. 3 PCSK9 inhibitor downregulates miR-130a-3p to promote LDLR expression. HepG2 cells or miR-130a-3p mimics-transfected HepG2 cells were treated with PCSK9 inhibitor, then total RNAs and protein were collected for experiments. **A** The expression of miR-130a-3p was assessed by qRT-PCR. **B** The expression of LDLR mRNA was assessed by qRT-PCR. **C** The expression of LDLR protein was assessed by western blot. atherosclerosis model mice were treated with PCSK9 inhibitor, or co-treated with PCSK9 inhibitor and AAV-control or AAV-miR-130a-3p, then total RNAs and protein of liver tissues were collected for experiments. **D** The expression of miR-130a-3p was assessed by qRT-PCR. **E** The expression of LDLR mRNA was assessed by qRT-PCR. **F** Expression and co-localization of LDLR mRNA and miR-130a-3p in liver tissues were observed via immunofluorescence staining. Scale bar: 50 um. Data present mean ± SEM from three independent experiments at least. $^{***}P < 0.001$, compared with the control groups. $^{**}P < 0.01$; $^{***}P < 0.001$

levels were decreased in atherosclerosis model mice. Compared with the model, the levels of serum TG, TC, and LDL-C in the PCSK9 inhibitor group were significantly decreased, and HDL-C levels were significantly increased. However, as shown in Fig. 5, AAV-miR-130a-3p co-treatment reversed the levels of serum TG, TC, LDL-C, and HDL-C.

PCSK9 inhibitor restrains atherosclerosis progression in atherosclerosis mice via regulation of miR-130a-3p

First, we measured the size of plaque lesions in the entire aorta of each group of mice. As shown by the Oil Red O-staining, no plaque lesions were observed in the control

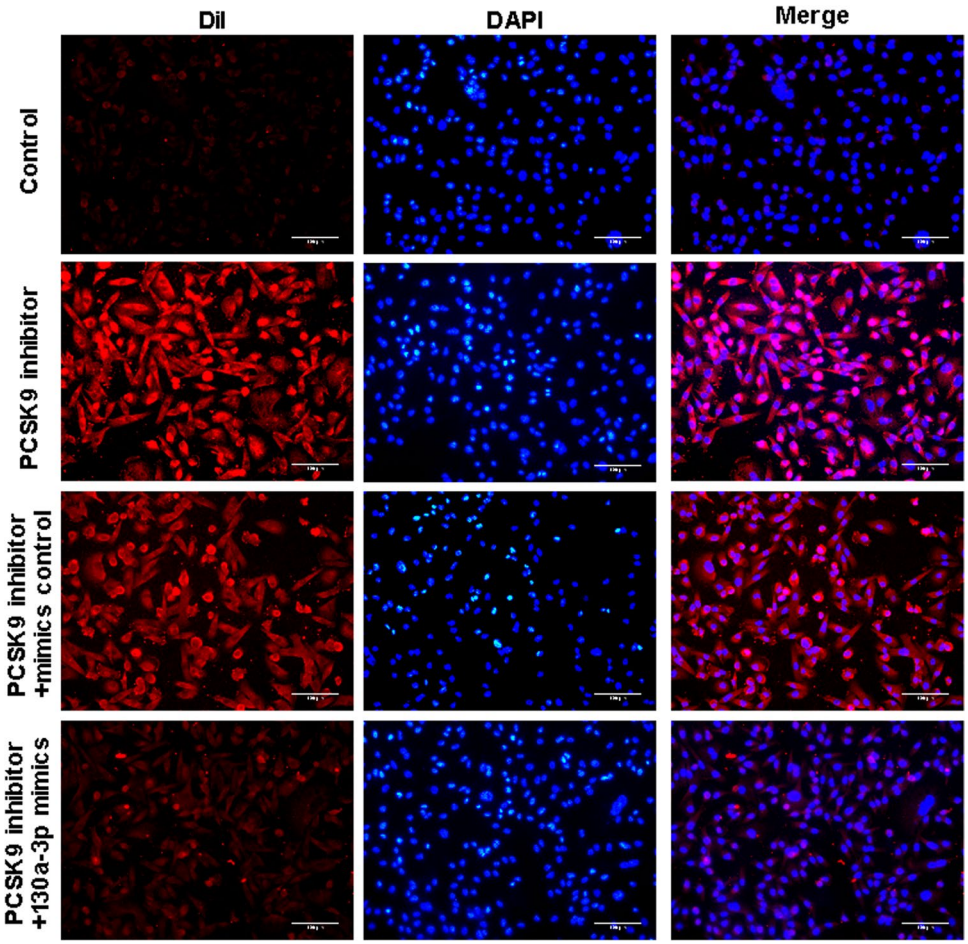

Fig. 4 PCSK9 inhibitor promotes DiI-LDL uptake in HepG2 cells via regulation of miR-130a-3p. Scale bar: 100 um

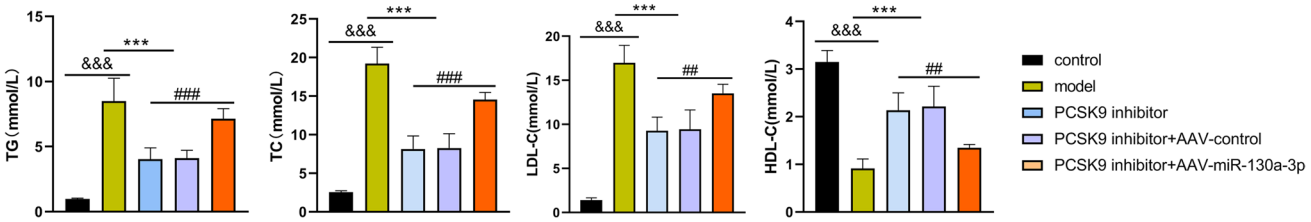

Fig. 5 PCSK9 inhibitor regulates serum TG, TC, LDL-C, and HDL-C in atherosclerosis mice via downregulation of miR-130a-3p

group, while significant plaque lesions were observed in the whole aorta of the model group. However, plaque lesions in the mice were reduced after PCSK9 inhibitor treatment. Mice treated with AAV-miR-130a-3p had more plaque lesions than those treated with PCSK9 inhibitor alone (Fig. 6A).

Since the burden of atherosclerotic plaque in the aortic sinus is another important indicator to evaluate the severity of atherosclerosis, the HE-stained paraffin sections of the aortic sinus were analyzed. As shown by H&E staining, there were no plaques in the control group, while there were a large number of plaques under the intima of the model group with significant plaque thickening. PCSK9 inhibitors significantly reduced the atherosclerotic plaque area in the cross-section of the aortic sinus. Concurrent treatment with AAV-miR-130a-3p attenuated this therapeutic effect of PCSK9 inhibitors (Fig. 6B).

As shown in the ORO-stained frozen section of Fig. 6C, the nuclei were blue and the atherosclerotic adipose region was red under an inverted microscope. Plaques were observed in the control group, and extensive and typical atherosclerotic mature plaques were found in the model group. Fatty plaques were significantly reduced after PCSK9 inhibitor intervention. However, the adipose plaque increased after co-treatment with AVV compared with the PCSK9 inhibitor group.

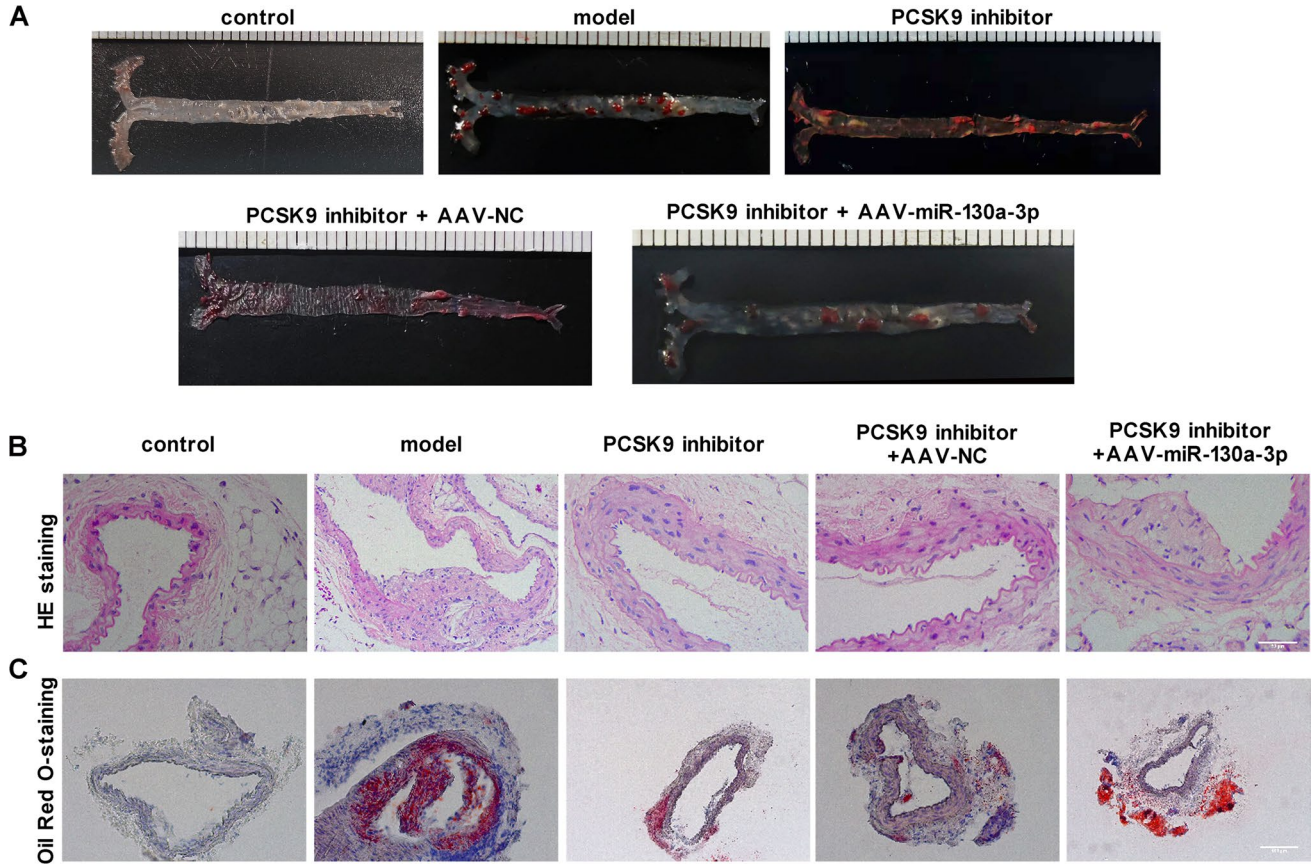

Fig. 6 PCSK9 inhibitor restrains atherosclerosis progression in atherosclerosis mice via downregulation of miR-130a-3p. Atherosclerosis model mice were treated with PCSK9 inhibitor, or co-treated with PCSK9 inhibitor and AAV-control or AAV-miR-130a-3p, and then the aortas of mice were collected for experiments. **A** Oil Red O-staining was used to measure the size of plaque lesions in the entire aorta. **B** HE-stained paraffin sections of the aortic sinus were analyzed. Scale bar: 50 um. **C** Fatty plaques in the ORO-stained frozen section were evaluated. Scale bar: 100 um

Discussion

PCSK 9 has been identified as a key participant in lipid metabolism, playing an important role in the development and progression of atherosclerosis (Seidah and Prat 2022). Understanding the biology of PCSK9 has stimulated scientists' interest in PCSK9 inhibitors. Although the primary effects of PCSK9 inhibitors are mediated by upregulation of LDLR protein and subsequent regulation of circulating cholesterol levels, increasing evidence indicates that PCSK9 may be pleiotropic (Ding et al. 2020a, b). In the present study, we confirmed that the PCSK9 inhibitor inhibited miR-130a-3p to increase LDLR expression in hepatic cells. In addition, overexpression of miR-130a-3p could reverse the effects of PCSK9 inhibitor on DiI-LDL uptake function of hepatic cells, serum lipids, and atherosclerosis progression in mice. Our study expounded that PCSK9 inhibitor could regulate lipid metabolism and prevents atherosclerosis progress by the miR-130a-3p/LDLR axis, laying the foundation for its clinical application.

Numerous clinical trials have demonstrated that PCSK9 inhibitors significantly reduce LDL cholesterol levels and cardiovascular events (Hao et al. 2022). However, there are few studies on its mechanism. PCSK9 is a multifunctional protein. In addition to the classical efficacy of LDLR regulation, PCSK9 is also involved in the regulation of other molecular or biological events (Guo et al. 2022). For example, PCSK9 induces the secretion of pro-inflammatory cytokines in macrophages, hepatocytes, and other various tissues (Wu et al. 2022). PCSK9 regulates toll-like receptor 4 expression, NF-κB activation, apoptosis, and autophagy development (Scalise and Sanguinetti 2021). PCSK9 also interacts with oxidized low-density lipoprotein receptor 1 (LOX-1) in a mutually promoting manner (Ding et al. 2020a, b). Therefore, we speculated that PCSK9 inhibitors might be pleiotropic. MiRNAs are a kind of short, non-coding RNAs and participate in a variety of biological processes. A large number of studies have shown that miRNAs are involved in lipid metabolism and atherosclerosis progression (Huang et al. 2021; Yu et al. 2022). For example, several studies have

revealed that miR-552-3p, miR-483, and miR-337-3p lower serum LDL-C levels and ameliorate hypercholesterolemia by targeting PCSK9 (Dong et al. 2020; Ma et al. 2021; Xu et al. 2021). Here, we observed that miR-130a-3p was significantly upregulated in atherosclerosis mice. However, PCSK9 inhibitor could significantly reduce miR-130a-3p expression in liver cells and liver tissues of atherosclerosis mouse. Moreover, overexpression of miR-130a-3p could reverse the effects of PCSK9 inhibitor on DiI-LDL uptake function of hepatic cells, serum lipids and atherosclerosis progression in mice. Collectively, these data confirmed the involvement of miR-130a-3p in PCSK9 inhibitor-mediated lipid metabolism.

MiR-130a-3p has been reported to be implicated in various hepatic diseases. A previous study showed that miR-130a-3p induced hepatic stellate cell apoptosis in nonalcoholic fibrosing steatohepatitis by suppressing TGFBR1 and TGFBR2 (Wang et al. 2017). MiR-130a-3p alleviates liver fibrosis by suppressing HSCs activation and skewing macrophages to Ly6Clo phenotype (Liu et al. 2021). Hepatic exosome-derived miR-130a-3p attenuates glucose intolerance via directly targeting the PHLPP2 gene in adipocytes (Wu et al. 2020). As for how miR-130a-3p affects lipid metabolism, here, we found that miR-130a-3p negatively regulated the expression of LDLR, and further confirmed the binding of miR-130a-3p to LDLR by luciferase assay. LDLR recognizes, binds, and internalizes circulating cholesterol-containing lipoprotein particles, including VLDL, IDL, HDL, and chylomicron remnant, maintaining cholesterol homeostasis in mammals (Ji et al. 2021). Abnormal expression or dysfunction of LDLR causes dyslipidemia, which has been considered an underlying cause of coronary artery diseases (Chang et al. 2021). Thus, we concluded that upregulated miR-130a-3p affects serum lipid maintenance by inhibiting LDLR. Indeed, our study revealed miR-130a-3p overexpression attenuated PCSK9 inhibitor-mediated protective effect on lipid metabolism and atherosclerosis progression in atherosclerosis mice. Thus, we confirmed that PCSK9 inhibitors restore lipid disorders and protect against atherosclerosis progression through miR-130a-3p /LDLR axis.

Conclusion

Collectively, we demonstrated that PCSK9 inhibitor could moderately restore lipid disorders and prevent the progression of atherosclerosis by inhibiting miR-130a-3p to upregulate LDLR expression. This study provides the basis for the application of PCSK9 inhibitors to prevent atherosclerosis and associated clinical events.

Author contributions J.X. and J.Z. wrote the main manuscript text. C.H. and T.L. prepared Figs. 1, 2 and 3. J.Z. and F.Z. prepared Figs. 4 and 5. J.X., D.J. and H.C. prepared Fig. 6. All authors reviewed the manuscript. The authors declare that all data were generated in-house and that no paper mill was used.

Funding This study was funded by the Science and Technology Plan Projects of Tianjin Jinnan district (No. 20190104) and Tianjin Key Medical Discipline(specialty) Construction Project [Internal Medicine (Cardiology):TJYXZDXK-055B].

Data availability The datasets used and/or analyzed during the current study are available from the corresponding author on reasonable request.

Declarations

Competing interests The authors declare no competing interests.

Ethics approval All experiments were approved and conducted by the ethics committee of Tianjin Chest Hospital (TJCH-2021-009).

Disclosure No potential competing interest was reported by the authors.

References

Agbu P, Carthew RW (2021) MicroRNA-mediated regulation of glucose and lipid metabolism. Nat Rev Mol Cell Biol 22(6):425–438

Aguilar-Salinas CA, Gómez-Díaz RA (2021) New therapies for primary hyperlipidaemia. J Clin Endocrinol Metab 107(5):1216–1224

Chang X, Lochner A, Wang HH, Wang S, Zhu H, Ren J, Zhou H (2021) Coronary microvascular injury in myocardial infarction: perception and knowledge for mitochondrial quality control. Theranostics 11(14):6766–6785

Ding Z, Pothineni NVK, Goel A, Lüscher TF, Mehta JL (2020a) PCSK9 and inflammation: role of shear stress, pro-inflammatory cytokines, and LOX-1. Cardiovasc Res 116(5):908–915

Ding Z, Pothineni NVK, Goel A, Lüscher TF, Mehta JL (2020b) PCSK9 and inflammation: role of shear stress, pro-inflammatory cytokines, and LOX-1. Int J Mol Sci 116(5):908–915

Dong J, He M, Li J, Pessentheiner A, Wang C, Zhang J, Sun Y, Wang WT, Zhang Y, Liu J, Wang SC, Huang PH, Gordts PL, Yuan ZY, Tsimikas S, Shyy JY (2020) microRNA-483 ameliorates hypercholesterolemia by inhibiting PCSK9 production. JCI Insight 5(23):e143812

Förstermann U, Xia N, Li H (2017) Roles of vascular oxidative stress and nitric oxide in the pathogenesis of atherosclerosis. Circ Res 120(4):713–735

Guo Y, Tang Z, Yan B, Yin H, Tai S (2022) PCSK9 (Proprotein Convertase Subtilisin/Kexin Type 9) triggers vascular smooth muscle cell senescence and apoptosis: implication of its direct role in degenerative vascular disease. Arterioscler Thromb Vasc Biol 42(1):67–86

Hao Q, Aertgeerts B, Guyatt G, Bekkering GE, Vandvik PO, Khan SU, Rodondi N, Jackson R, Reny JL, Al Ansary L, Van Driel M, Assendelft WJJ, Agoritsas T, Spencer F, Siemieniuk RAC, Lytvyn L, Heen AF, Zhao Q, Riaz IB, Ramaekers D, Okwen PM, Zhu Y, Dawson A, Ovidiu MC, Vanbrabant W, Li S, Delvaux N (2022) PCSK9 inhibitors and ezetimibe for the reduction of cardiovascular events: a clinical practice guideline with risk-stratified recommendations. Endocr Rev 377:e069066

Hilvo M, Dhar I (2022) Primary cardiovascular risk prediction by LDL-cholesterol in Caucasian middle-aged and older adults: a joint analysis of three cohorts. Eur J Prev Cardiol 29(3):e128–e137

Huang M, Wang YZ, Lu J (2021) microRNA-378b regulates ethanol-induced hepatic steatosis by targeting CaMKK2 to mediate lipid metabolism. Bioengineered 12(2):12659–12676

Ji J, Feng M, Niu X, Zhang X, Wang Y (2021) Liraglutide blocks the proliferation, migration and phenotypic switching of Homocysteine (Hcy)-induced vascular smooth muscle cells (VSMCs) by suppressing proprotein convertase subtilisin kexin9 (PCSK9)/low-density lipoprotein receptor (LDLR). Bioengineered 12(1):8057–8066

Jiang G, Sun C, Wang X, Mei J, Li C, Zhan H, Liao Y, Zhu Y, Mao J (2022) Hepatoprotective mechanism of Silybum marianum on nonalcoholic fatty liver disease based on network pharmacology and experimental verification. Bioengineered 13(3):5216–5235

Leal K, Saavedra K, Rebolledo C, Salazar LA (2021) MicroRNAs hsa-miR-618 and hsa-miR-297 might modulate the pleiotropic effects exerted by statins in endothelial cells through the inhibition of ROCK2 kinase: in-silico approach. Front Cardiovasc Med 8:704175

Liu L, Wang P, Wang YS, Zhang YN, Li C, Yang ZY, Liu ZH, Zhan TZ, Xu J, Xia CM (2021) MiR-130a-3p alleviates liver fibrosis by suppressing HSCs activation and skewing macrophage to Ly6C(lo) phenotype. Front Immunol 12:696069

Liu Y, Luo G, Tang Q, Song Y, Liu D, Wang H, Ma J (2022) Methyltransferase-like 14 silencing relieves the development of atherosclerosis via m(6)A modification of p65 mRNA. Bioengineered 13(5):11832–11843

Ma N, Fan L, Dong Y, Xu X, Yu C, Chen J, Ren J (2021) New PCSK9 inhibitor miR-552-3p reduces LDL-C via enhancing LDLR in high fat diet-fed mice. Pharmacol Res 167:105562

Oleaga C, Shapiro MD, Hay J, Mueller PA, Miles J, Huang C, Friz E, Tavori H, Toth PP, Wójcik C, Warden BA, Purnell JQ, Duell PB, Pamir N, Fazio S (2021) Hepatic sensing loop regulates PCSK9 secretion in response to inhibitory antibodies. J Am Coll Cardiol 78(14):1437–1449

Sánchez-Bacaicoa C, Galán J, Guijarro C (2022) Sustained low-density lipoprotein-cholesterol <70 mg/dl is associated with improved cardiovascular outcomes in the clinical setting. Eur J Clin Invest 52(5):e13732

Saavedra K, Leal K, Saavedra N, Prado Y, Paez I, Ubilla CG, Rojas G, Salazar LA (2022) MicroRNA-20a-5p downregulation by atorvastatin: a potential mechanism involved in lipid-lowering therapy. Int J Mol Sci 23(9):5022. https://doi.org/10.3390/ijms23095022

Scalise V, Sanguinetti C (2021) PCSK9 induces tissue factor expression by activation of TLR4/NFkB signaling. Int J Mol Sci 22(23):12640

Seidah NG, Prat A (2022) The multifaceted biology of PCSK9. Endocr Rev 43(3):558–582

Suvorov A, Naumov V, Shtratnikova V, Logacheva M, Shershebnev A, Wu H, Gerasimov E, Zheludkevich A, Pilsner JR, Sergeyev O (2020) Rat liver epigenome programing by perinatal exposure to 2,2',4'4'-tetrabromodiphenyl ether. Epigenomics 12(3):235–249

Ubilla CG, Prado Y, Angulo J, Obreque I, Paez I, Saavedra N, Saavedra K, Zambrano T, Salazar LA (2021) MicroRNA-33b is a potential non-invasive biomarker for response to atorvastatin treatment in chilean subjects with hypercholesterolemia: a pilot study. Front Pharmacol 12:674252

Wang Y, Du J, Niu X, Fu N, Wang R, Zhang Y, Zhao S, Sun D, Nan Y (2017) MiR-130a-3p attenuates activation and induces apoptosis of hepatic stellate cells in nonalcoholic fibrosing steatohepatitis by directly targeting TGFBR1 and TGFBR2. Cell Death Dis 8(5):e2792

Wu J, Dong T, Chen T, Sun J, Luo J, He J, Wei L, Zeng B, Zhang H, Li W, Liu J, Chen X, Su M, Ni Y, Jiang Q, Zhang Y, Xi Q (2020) Hepatic exosome-derived miR-130a-3p attenuates glucose intolerance via suppressing PHLPP2 gene in adipocyte. Metabolism 103:154006

Wu NQ, Shi HW, Li JJ (2022) Proprotein convertase subtilisin/kexin type 9 and inflammation: an updated review. Front Cardiovasc Med 9:763516

Xiao F, Yu J, Liu B, Guo Y, Li K, Deng J, Zhang J, Wang C, Chen S, Du Y, Lu Y, Xiao Y, Zhang Z, Guo F (2014) A novel function of microRNA 130a–3p in hepatic insulin sensitivity and liver steatosis. Diabetes 63(8):2631–2642

Xu X, Dong Y, Ma N, Kong W, Yu C, Gong L, Chen J, Ren J (2021) MiR-337-3p lowers serum LDL-C level through targeting PCSK9 in hyperlipidemic mice. Metabolism 119:154768

Yu Y, Tian T, Tan S, Wu P, Guo Y, Li M (2022) MicroRNA-665-3p exacerbates nonalcoholic fatty liver disease in mice. Bioengineered 13(2):2927–2942

Zhou W, Yang F (2022) Circular RNA circRNA-0039459 promotes the migration, invasion, and proliferation of liver cancer cells through the adsorption of miR-432. Bioengineered 13(5):11810–11821